I. Torrini,[1]
M. Paglialunga Paradisi,[1]
G. Pagani Zecchini,[1]
G. Lucente,[1]
E. Gavuzzo,[2]
F. Mazza,[2,3]
G. Pochetti,[2]
S. Traniello,[4]
S. Spisani[4]

[1] *Dipartimento di Studi Farmaceutici and Centro di Studio per la Chimica del Farmaco del CNR, Università La Sapienza, 00185 Roma, Italy*

[2] *Istituto di Strutturistica Chimica G. Giacomello, CNR, 00016 Monterotondo Stazione, Roma, Italy*

[3] *Dipartimento di Chimica, Università di L'Aquila, 67010 L'Aquila, Italy*

[4] *Dipartimento di Biochimica e Biologia Molecolare, Università di Ferrara, 44100 Ferrara, Italy*

Synthesis, Conformation, and Biological Activity of Two fMLP-OMe Analogues Containing the New 2-[2′-(Methylthio)ethyl]methionine Residue

Received 14 June 1996; accepted 27 March 1997

Abstract: *The new C^{α}-tetrasubstituted α-amino acid residue 2-[2′-(methylthio)ethyl]methionine (Dmt) has been introduced into the reference chemotactic tripeptide HCO-Met-Leu-Phe-OMe (fMLP-OMe) in place of the leucine or methionine, respectively. The biological activity of the new analogues [Dmt^2]fMLP-OMe (**2**) and [Dmt^1]fMLP-OMe (**3**) has been determined; whereas **2** is active toward human neutrophils, stimulating directed migration, superoxide anion generation, and lysozyme release, **3** results practically inactive in all tested assays. A conformational analysis on **2** and **3** has been performed in solution by using ir absorption and ^{1}H-nmr. The conformation of **2** was also examined in the crystal by x-ray diffraction methods. Both **2** and **3** adopt fully extended conformation in correspondence with the Dmt residue. Biological and conformational results are discussed and compared with related previously studied models.* © *1997 John Wiley & Sons, Inc. Biopoly* ***42:*** *415–426, 1997*

Keywords: *chemotaxis; conformation; crystal structure; C^{α}-tetrasubstituted amino acids; formylpeptides; 2-[2′-(methylthio)ethyl]methionine*

Correspondence to: G. Lucente
Contract grant sponsor: Ministero dell'Università e della Ricerca Scientifica e Tecnologica (MURST)

CCC 0006-3525/97/040415-12

INTRODUCTION

Incorporation of C^{α}-tetrasubstituted α-amino acids into the peptide backbone represents one of the most effective strategies to restrict the available range of backbone conformations.[1–4] In this context we recently reported the synthesis and properties of *N*- and *C*-protected derivatives of the new $C^{\alpha,\alpha}$-dialkyl substituted residue 2-[2′-(methylthio)ethyl]methionine (Dmt; **1**).[5] This achiral α-amino acid was designed in order to combine the tendency of the C^{α}-tetrasubstituted residues to introduce conformational constraint into the peptide backbone with the maintenance of the chemical and binding properties which are specific of the methionine side chain.

As a prosecution of previous studies on the chemical modification of bioactive peptides, we report here the results of the incorporation of Dmt into the backbone of the prototypical chemotactic tripeptide HCO-Met-Leu-Phe-OMe (fMLP-OMe). In order to further investigate the role of both the backbone conformation and the side chain topography on the biological activity of this highly active chemotactic agent, the two modified analogues HCO-Met-Dmt-Phe-OMe (**2**) and HCO-Dmt-Leu-Phe-OMe (**3**) have been synthesized. In the analogue **2** the C^{α}-tetrasubstituted residue has been located at the central position in place of the leucine. This modification should give information on the tendency of the new residue to stabilize extended conformations, as it is the case of α,α-disubstituted glycine residues containing linear side chains longer than methyl groups.[6] It should be also noted, in this context, that a recently described fMLP-OMe analogue, containing the $C^{\alpha,\alpha}$-di-*n*-propylglycine (Dpg) residue at the central position, adopts an extended conformation and exhibits high chemotactic activity.[7]

The analogue **3** contains the new residue located at the *N*-terminal position, so as to mimic the role of the native methionine whose key role in the interaction with the *N*-formylpeptide receptors is well established. To our best knowledge, this is the first fMLP-OMe analogue that contains a *N*-terminal residue with two linear side chains bound at the C^{α} atom.

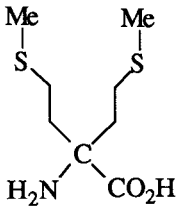

Dmt (**1**)

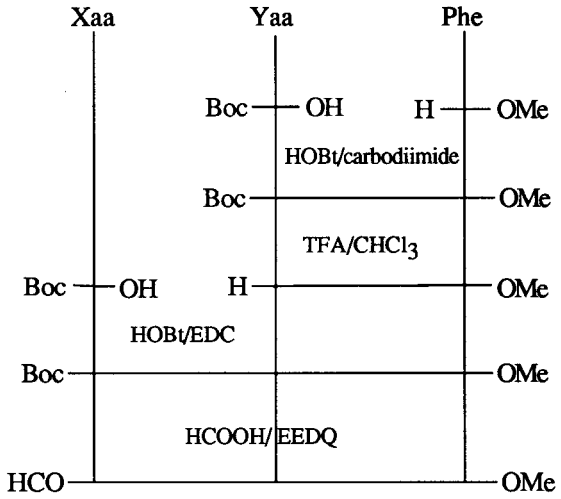

2: Xaa = Met, Yaa = Dmt

3: Xaa = Dmt, Yaa = Leu

SCHEME 1

RESULTS AND DISCUSSION

Synthesis

The formyltripeptides **2** and **3**, containing the Dmt (**1**) residue at the central and *N*-terminal position, respectively, were synthesized according to Scheme 1. The intermediate peptides Boc-Dmt-Phe-OMe, Boc-Met-Dmt-Phe-OMe, and Boc-Dmt-Leu-Phe-OMe were prepared by coupling Boc-Dmt-OH[5] and Boc-Met-OH with the appropriate residue by the 1-hydroxybenzotriazole (HOBt)/*N*-(3-dimethylaminopropyl)-*N*′-ethylcarbodiimide hydrochloride (EDC) method. Boc-Leu-Phe-OMe was obtained using *N*,*N*′-dicyclohexylcarbodiimide (DCC) as previously described.[8] Deprotection of Boc-dipeptides Boc-Dmt-Phe-OMe and Boc-Leu-Phe-OMe was performed with trifluoroacetic acid (TFA)-$CHCl_3$. Finally, treatment of Boc-tripeptide methyl esters with HCOOH followed by *N*-ethoxycarbonyl-2-ethoxy-1,2-dihydroquinoline (EEDQ)[9] afforded the *N*-formyltripeptides **2** and **3.**

Molecular Structure of 2

The molecular conformation adopted in the crystal by the *N*-formyltripeptide **2** bis-benzene solvate together with the numbering scheme are shown in Figure 1 while the relevant torsion angles are reported in Table I. The two peptide bonds are *trans*

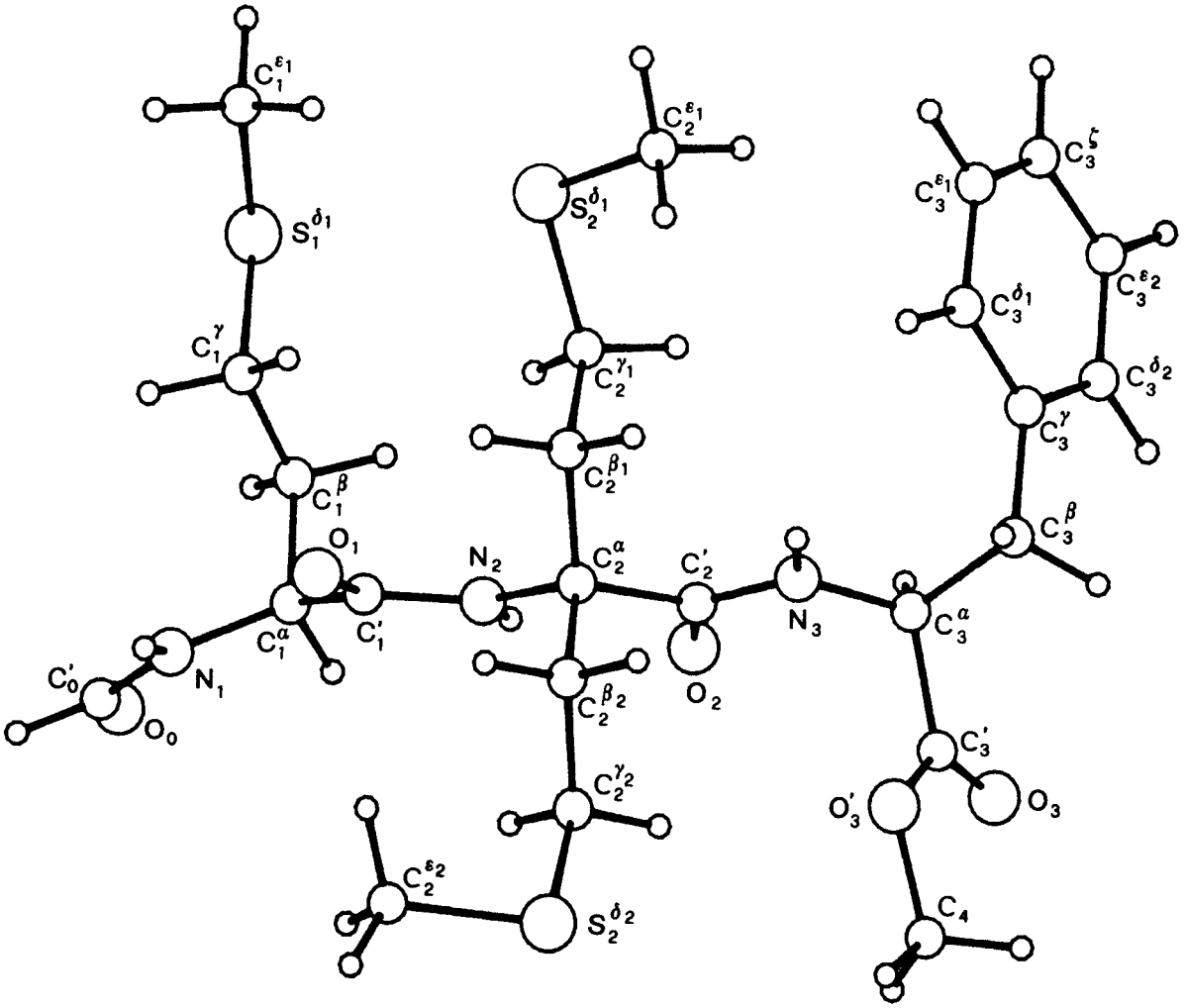

FIGURE 1 Molecular conformation (occupancy factor 0.67) found in the crystal of **2**.

and the largest deviation from planarity occurs at the Met-Dmt junction ($\omega_1 = 174.2°$). The formamido group is planar with the Met C_1^{α} and the carbonylic oxygen O_0 on one side of the C_0'-N_1 bond and the two hydrogen atoms on the other side. This atomic arrangement is that always observed in the crystal structures of *N*-formylpeptides.[10]

The peptide backbone is extended with a twist at the *C*-terminal Phe residue. In particular, the novel Dmt residue adopts a fully extended conformation with ϕ and ψ values of $-179.0°$ and 171.7° giving rise to the C_5 structure characterized by the τ (N_2-C_2^{α}-C_2') angle of 103.5°, markedly smaller than the tretrahedric value, and by short contacts between the NH and CO groups ($N\cdots O = 2.551$ Å, $H\cdots O = 2.04$ Å). C_5 structures have been observed in the crystals of oligopeptides incorporating related α,α-dialkylated residues with acyclic side chains longer that methyl groups.[6,11] The twist observed at the *C*-terminal Phe residue is described by the pertinent ϕ_3 and ψ_T values of $-74°$ and $-32°$, respectively (see Table I).

Two different arrangements of the Met side chain are observed. The Met side chain with the larger occupancy factor adopts the g^+, *t*, *t* conformation; that with lower occupancy factor differs for the g^+ orientation of the terminal methyl group; χ^3 values corresponding to the *t* conformation are those most frequently observed in the structures of oligopeptides containing unbranched side chains.[12] The conformation of the two side chains of the Dmt residue is g^-, *t*, g^+ and g^+, *t*, g^+ for that facing the Met side chain and the ester group, respectively. The Phe χ^1 corresponds to the g^- rotameric conformation while the aromatic ring adopts the usual orientation characterized by $\chi^2 \sim \pm 90°$.[13,14]

The structure of the peptide under study can be compared with that of the fMLP-OMe analogue

Table I Relevant Torsion Angles (°) of 2

Backbone		
O_0-C'_0-N_1-C^{α}_1	$\theta^{0'}$	−1(2)
C'_0-N_1-C^{α}_1-C'_1	ϕ^1	−162(1)
N_1-C^{α}_1-C'_1-N_2	ψ_1	154.7(9)
C^{α}_1-C'_1-N_2-C^{α}_2	ω_1	174.2(8)
C'_1-N_2-C^{α}_2-C'_2	ϕ_2	−179.0(9)
N_2-C^{α}_2-C'_2-N_3	ψ_2	171.7(7)
C^{α}_2-C'_2-N_3-C^{α}_3	ω_2	172.3(8)
C'_2-N_3-C^{α}_3-C'_3	ϕ_3	−74(1)
N_3-C^{α}_3-C'_3-O'_3	ψ_T	−32(1)
C^{α}_3-C'_3-O'_3-C_4	ω_T	−175(1)
Met side chain		
N_1-C^{α}_1-C^{β}_1-C^{γ}_1	χ^1_1	58(2)
C^{α}_1-C^{β}_1-C^{γ}_1-$S^{\delta 1}_1$	$\chi^{2,1a}_1$	−179(1)
C^{β}_1-C^{γ}_1-$S^{\delta 1}_1$-$C^{\epsilon 1}_1$	$\chi^{3,1a}_1$	−159(2)
C^{α}_1-C^{β}_1-C^{γ}_1-$S^{\delta 2}_1$	$\chi^{2,2b}_1$	147(2)
C^{β}_1-C^{γ}_1-$S^{\delta 2}_1$-$C^{\delta 2}_1$	$\chi^{3,2b}_1$	54(3)
Dmt side chains		
N_2-C^{α}_2-$C^{\beta 1}_2$-$C^{\gamma 1}_2$	$\chi^{1,1}_2$	−60(1)
C^{α}_2-C^{β}_2-$C^{\gamma 1}_2$-$S^{\delta 1}_2$	$\chi^{2,1}_2$	166.9(8)
$C^{\beta 1}_2$-$C^{\gamma 1}_2$-$S^{\delta 1}_2$-$C^{\epsilon 1}_2$	$\chi^{3,1}_2$	75(1)
N_2-C^{α}_2-$C^{\beta 2}_2$-$C^{\gamma 2}_2$	$\chi^{1,2}_2$	57(1)
C^{α}_2-$C^{\beta 2}_2$-$C^{\gamma 2}_2$-$S^{\delta 2}_2$	$\chi^{2,2}_2$	−174.6(9)
$C^{\beta 2}_2$-$C^{\gamma 2}_2$-$S^{\delta 2}_2$-$C^{\epsilon 2}_2$	$\chi^{3,2}_2$	75(1)
Phe side chain		
N_3-C^{α}_3-C^{β}_3-C^{γ}_3	χ^1_3	−80(1)
C^{α}_3-C^{β}_3-C^{γ}_3-$S^{\delta 1}_3$	$\chi^{2,1}_3$	88(2)
C^{α}_3-C^{β}_3-C^{γ}_3-$S^{\delta 2}_3$	$\chi^{2,2}_3$	−91(2)

[a] Atoms $S^{\delta 1}_1$ and $C^{\epsilon 1}_1$ have an occupancy factor of 0.67.
[b] Atoms $S^{\delta 2}_1$ and $C^{\epsilon 2}_1$ have an occupancy factor of 0.33.

previously studied by Dentino et al., containing the achiral Dpg residue in place of the central leucine.[7] A comparison between the conformations adopted in the crystal by the two *N*-formyltripeptides reveals that in both models the backbone is fully extended at the central residue and (differently) folded at the *C*-terminal phenylalanine. However, the backbone conformation at the *N*-terminal methionine differs in the two analogues, being almost fully extended in the peptide under study (ϕ_1, $\psi_1 = -162°$, 154.7°) and folded in the Dpg containing model (ϕ_1, $\psi_1 = -75.8°$, −30.4°). This different backbone conformation is accompanied by a different spatial orientation of the Met and Phe side chains with respect to the backbone plane; in particular, the two chains are on the same side in the case of the Dmt analogue **2** (see Figure 1) and on the opposite side in the case of the Dpg containing formyltripeptide.[7]

Crystal Packing

Two intermolecular H bonds characterize the packing of peptide molecules; the N_2 of the reference molecule forms a weak H bond with the carbonylic O_3 of a screw-related molecule while the N_3 is engaged with the formylic O_0 of the peptide translated by a *b* unit. The contacts and angles are as follows: $N_2 \cdots O_3 = 3.141(5)$ Å, $H_2 \cdots O_3 = 2.27(2)$ Å, N_2-$H_2 \cdots O_3 = 136(1)°$ and $N_3 \cdots O_0 = 2.985(5)$ Å, $H_3 \cdots O_0 = 1.92(2)$ Å, N_3-$H_3 \cdots O_0 = 167(1)°$. The packing of peptides is completed by van der Waals interactions, the closest contacts being formed between the C atoms of the Phe ring and the Met methyl groups.

The side chains of all three residues form hydrophobic channels, centered on the twofold screw axis at $a = \frac{1}{2}$, $c = 0$ and extended along the *b* direction, where the rings of the two cocrystallized benzene molecules alternate in a staircase fashion with their planes almost perpendicular to each other. A top and side view of the channels are given in Figure 2. Along the helical path the benzene rings form van der Waals interactions with all the methyl groups and with the Phe aromatic rings. The shortest contact between the C atoms of the two benzene rings is 4.04(2) Å.

^{1}H-NMR and IR Studies

The ^{1}H-nmr study of the formyltripeptide **2** has been performed in $CDCl_3$ and DMSO solutions. In $CDCl_3$ the characteristic H-CO proton resonance occurs as a singlet at 8.19 δ. The Dmt NH signal appears as a singlet at 7.34 δ; the Met and Phe NH protons resonate as superimposed signals at 6.34 δ. Addition of a small amount (1%) of $(CD_3)_2SO$ to the $CDCl_3$ solution of **2** allows the separation of the Phe NH resonance (doublet at 7.07 ppm, $J = 8.2$ Hz) from that of the Met NH (doublet at 6.81 ppm, $J = 7.5$ Hz).

The involvement of NH groups in intramolecular hydrogen bonds was evaluated on the basis of the chemical shift solvent dependence in $CDCl_3$-$(CD_3)_2SO$ mixtures and temperature-induced NH shift variation in $(CD_3)_2SO$. In the solvent titration experiment (Figure 3A) the Met and Phe NH show substantial downfield shifts ($\Delta\delta = 1.48$ and 1.76 ppm, respectively), while the Dmt NH group is practically unaffected by the change of the solvent composition to 10% DMSO ($\Delta\delta = 0.17$ ppm). In $(CD_3)_2SO$ the Met and Phe NH groups show the same temperature coefficient ($d\delta/dT$) (0.0048 ppm/K) and this value is significantly higher than that calculated for the Dmt group (0.0006 ppm/K; Figure 3B). These results clearly indicate that the Dmt NH is not accessible to the solvents and is presumably involved in intramolecular hydrogen bonding in both $CDCl_3$ and $(CD_3)_2SO$, while the Met and Phe NH groups are solvent exposed.

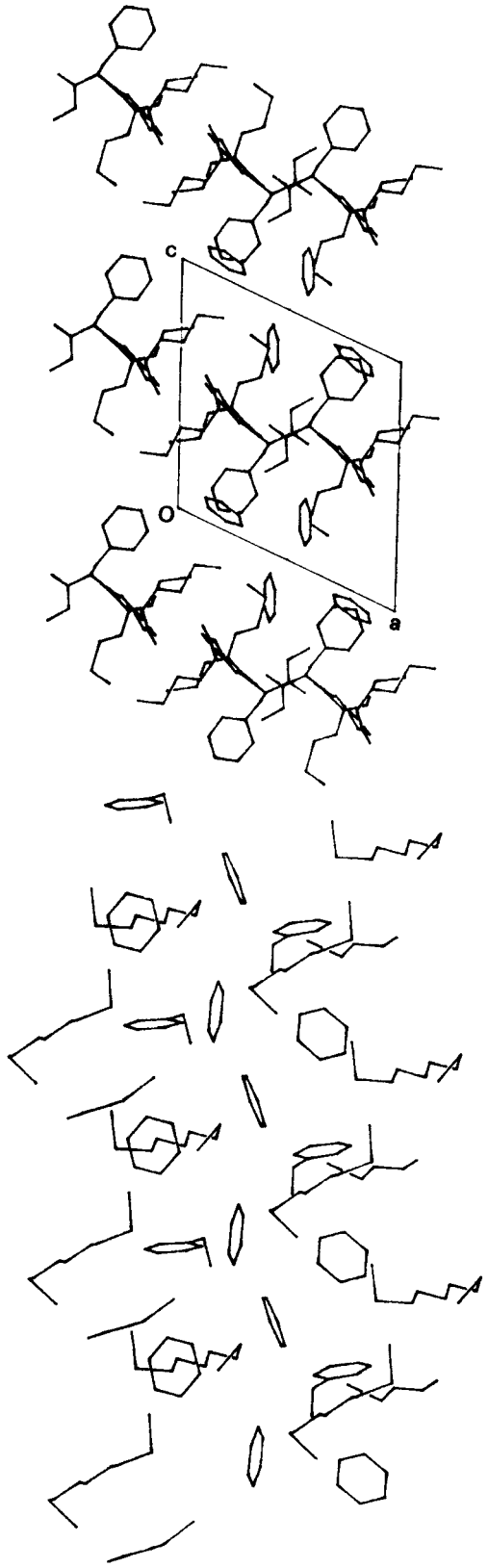

FIGURE 2 Top: crystal packing of **2** and top view of the hydrophobic channel centered at $a = \frac{1}{2}$, $c = 0$. Bottom: side view of the hydrophobic channel along the *b* axis; for clarity only the peptide side chains have been reported. The H atoms have been omitted in both figures.

Solution ir spectra have been examined in order to confirm the presence of intramolecularly H-bonded NH groups. Figure 4A shows the NH stretching region of the ir spectrum of **2** in $CHCl_3$. Two bands are observed at 3420 and 3358 cm^{-1}, corresponding to free (3420) and H-bonded (3358) NH groups. The ratio between the intensity of the free and H-bonded absorptions was found practically concentration independent over the range 10–0.3 m*M*. Thus, peptide self-association occurs, if any, to a limited extent under these experimental conditions and the band at 3358 cm^{-1} can be assigned to the intramolecularly H-bonded Dmt NH group.

It should be noted that the absorption associated with the NH stretching vibrators of C_5 type in peptide models containing C^{α}-tetrasubstituted residues is generally found at higher frequency (ca. 3400 cm^{-1}).[15,16] However, in the case of the fMLP-OMe analogue containing the Dpg residue at the central position recently described by Dentino et al.,[7] the fully extended C_5 conformation is found both in the crystal and in $CHCl_3$ solution, and the corresponding intramolecular NH absorption appears at the same frequency here observed for the related Dmt containing tripeptide **2.** The above discrepancy can be explained on the basis of the following consideration: although the position of the NH stretching bands of the ir spectra in solution gives valuable information on the presence of H-bonded conformations, its correlation with specific intramolecularly H-bonded peptide structures is not unequivocal. In accordance with this observation, several β-turn and γ-turn structures are found to be associated with NH-stretching bands positioned well inside the region which should be characteristic of C_5-type vibrators.[17–21] Thus, the peculiar structural and geometrical features characterizing the peptide turns as well the nature of the side chains and of the groups bonded to the CO and NH can sensibly enlarge the region where NH stretching vibrators appear, particularly when small ring systems are involved.

An analogous investigation of the preferred solution conformation in $CDCl_3$ solution has been performed on the [Dmt^1] analogue **3.** In the ^{1}H-nmr spectrum the H-CO resonance occurs as a singlet at 8.21 δ. The Dmt NH singlet appears at 6.95 δ and the Leu and Phe NH resonate as doublets at 6.46 δ (J = 7.5 Hz) and 6.29 δ (J = 7.3 Hz), respectively. The $(CD_3)_2SO$ titration results (Figure 3C) and the temperature-induced NH shift variation experiments (Figure 3D) suggest that the Dmt NH is involved in an intramolecular H bond, whereas the Leu and Phe NH are freely accessible to the solvent. These findings are supported by the ir spec-

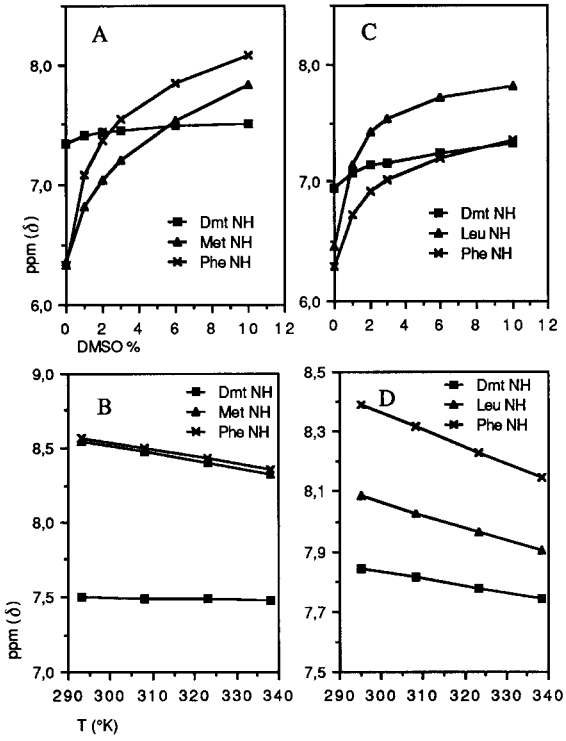

FIGURE 3 Delineation of hydrogen bonded NH groups in formyltripeptides **2** and **3**. Chemical shift dependence of the NH resonances as a function of the $(CD_3)_2SO$ concentration (% v/v) in $CDCl_3$ solution (A: **2**; C: **3**) and temperature dependence of NH chemical shifts in $(CD_3)_2SO$ (B: **2**; D: **3**). Peptide concentration 10 m*M*.

tral data in the NH stretching region (see Figure 4B), which reveal a behavior very similar (bands at 3420 and 3368 cm^{-1} for the free and H-bonded group, respectively) to that already evidenced in the case of the [Dmt^2] f MLP-OMe analogue **2.**

Examination of the above reported results suggests that both the tripeptide **2** and **3** adopt, in correspondence with the new Dmt residue, a fully extended C_5-ring structure stabilized by an intraresidue H bond. In the case of the [Dmt^1] analogue **3,** the solvent-exposed nature exhibited by both the Leu and Phe NH groups rules out any significant contribution by folded γ- or β-turn conformations involving the formylic carbonyl. Due to the free accessibility of the *C*-terminal Phe NH group, the same consideration holds true in the case of the [Dmt^2] model **2,** as far as the contribution of a β-turn structure is concerned. In this case, however, the existence of a γ-turn folding, centered at the *N*-terminal Met and stabilized by an intramolecular $3 \rightarrow 1$ H bond between the formylic carbonyl and the Dmt NH group, could be invoked to justify the low solvent accessibility shown by the NH of the central Dmt. This event appears quite improbable when the capacity of the Dmt residue to induce an extended C_5 conformation, evidenced in the case of the [Dmt^1] analogue, is considered together with the fully extended conformation at the central position found in the crystal of **2.** Furthermore, the $J_{NH\text{-}C^{\alpha}H}$ values observed for Met and Phe residues are very similar to those reported for the [Dpg^2] f MLP-OMe analogue, which has been shown to adopt an extended conformation.[7]

Biological Activity

The biological activity of the formylpeptides **2** and **3** has been determined on human neutrophils and compared with that of the parent tripeptide f MLP-OMe. Directed migration (chemotaxis), superoxide anion production, and lysozyme release have been measured. As shown in Figure 5, the analogue **2** is active, even if with a lesser potency than the standard peptide f MLP-OMe, as chemoattractant, segretagogue agent, and activator of the superoxide anion production. In contrast, **3** is unable to elicit all the tested biological responses. In particular, **2** is a chemotactic agent (Figure 5A) over a broad range of concentration (10^{-12}–$10^{-5}M$) with a peak at $10^{-9}M$; it elicits O_2^- production in a dose-dependent fashion having a peak at $10^{-7}M$ (Figure 5B), and it is a degranulation inducer in the concentration range of 10^{-8}–$10^{-5}M$ (Figure 5C).

Discussion and Conclusions

The two f MLP-OMe analogues **2** and **3**, containing the new Dmt residue at the central and *N*-terminal position, respectively, adopt extended backbone con-

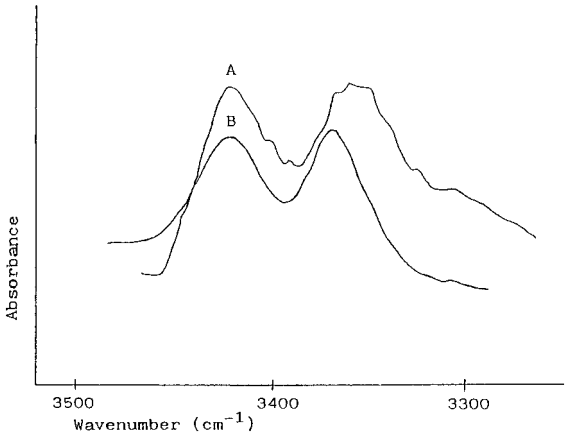

FIGURE 4 The ir absorption spectra (NH stretching bands) of **2** (A) and **3** (B) in chloroform. Concentration 1 m*M*, cells 2 mm.

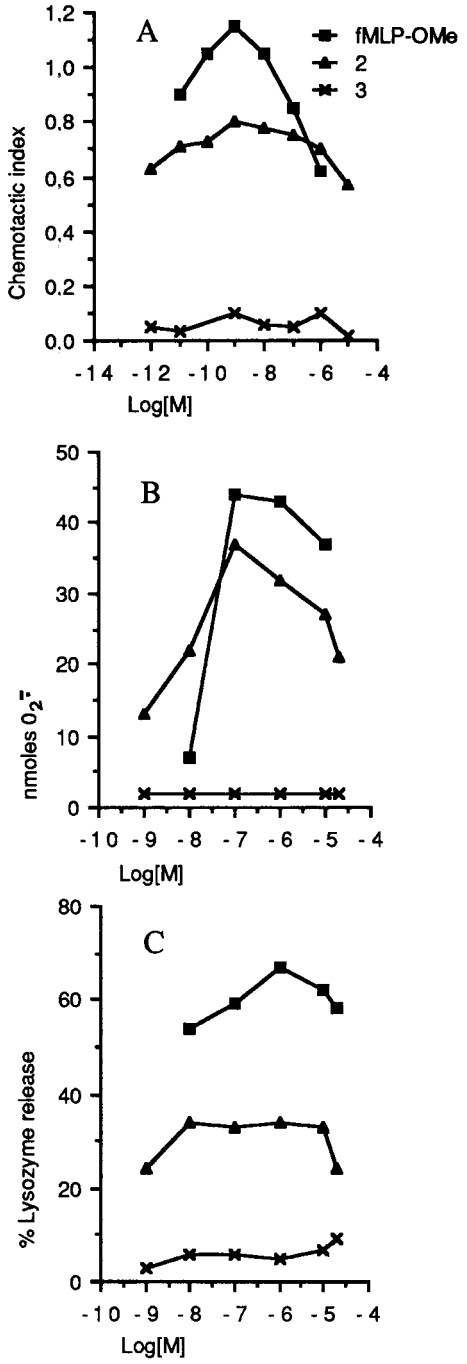

FIGURE 5. Biological activities of **2, 3,** and f MLP-OMe toward human neutrophils. (A) Chemotactic activity. The points are the mean of six separate experiments done in duplicate. Standard errors are in the 0.02–0.09 chemotactic index range. (B) Superoxide anion production. The points are the mean of six separate experiments done in duplicate. Standard errors are in the 0.1–4 nmoles O_2^- range. (C) Release of neutrophil granule enzymes evaluated by determining lysozyme activity. The points are the mean of five separate experiments done in duplicate. Standard errors are in the 1–6% range.

formation but exhibit different biological activity toward human neutrophils. In particular, the significant activity shown by the central substituted model **2** should be compared with the practically complete inactivity of the *N*-terminal substituted model **3.** The lack of activity shown by **3** can be reasonably ascribed to two different effects: the reduced availability of the formamido NH group, due to its involvement into an intramolecular H bond, and the steric interference associated with the presence of an additional side chain bound at the C^{α} atom of the *N*-terminal residue. Previous studies on the role of the formamido group clearly show the importance of this small moiety for specific binding interaction with the appropriate area of the receptor.[22–24] Some structural modifications, however, have been found compatible with the bioactivity,[25–27] and among these is the replacement of the NH with an oxygen atom (i.e., H-CO-O instead of H-CO-NH).[27] This finding suggests that the inactivity exhibited by the [Dmt^1] analogue **3** should be ascribed to the steric interference rather than to the intramolecular H bond involving the NH group. It is interesting to note that the negative steric effect prevails over the favorable conformation adopted by **3** in correspondence with the *N*-terminal residue; this is in fact extended as it is found for f MLP-OMe[28] and for f MLP-OH when cocrystallized with a protein resembling the neutrophil receptor.[23]

An examination of the backbone conformation found in the crystal reported in Figure 1 and of the corresponding ϕ_1, ψ_1 and ϕ_2, ψ_2 torsion angles of Table I shows that the analogue **2,** containing the Dmt residue at the central position, adopts an unusual backbone conformation exhibiting two consecutive extended residues. This feature can be evidenced by examining the backbone torsion angles of the chemotactic *N*-formyltripeptides studied so far that have been summarized in Table II. Only the prototypical chemotactic ligand f MLP-OMe exhibits a conformation extended at two residues; in this case, however, a folding occurs at the central Leu residue. Finally, the data reported in Table II clearly show that the sequence of ϕ and ψ torsion angles adopts values higher than 170° only in correspondence with the Dmt and Dpg residues. Thus, the here reported new α-amino acid, possessing two sulfur-containing side chains, maintains the relevant property, previously evidenced for Dpg and related C^{α}-tetrasubstituted residues, to stabilize, both in the solid state and in solution, a fully extended (C_5) conformation.[6]

The biological activity of the here studied [Dmt^2] analogue **2** parallels that found in the case of the related [Dpg^2] derivative.[7] The strong tendency of symmetrically $C^{\alpha,\alpha}$-dialkylsubstituted gly-

Table II Backbone Torsion Angles of Formyltripeptides[a]

Formyltripeptide	Torsion Angles (°)						Ref.
	ϕ_1	ψ_1	ϕ_2	ψ_2	ϕ_3	ψ_T	
For-Met-Leu-Phe-OMe	−146.0	151.3	−67.7	−49.1	−155.4	173.6	28
For-Met-Leu-Phe-O*t*Bu	−128.1	118.4	−98.8	114.1	−91.2	−176.3	29
For-Met-Leu-Ain-OMe[b]	−115	130	−127	125	61	27	30
	−137	145	−132	111	−62	−33	
For-Met-Leu-L-(αMe)Phe-OMe	−138.9	126.2	−107.4	122.3	−46.9	−48.7	31
For-Thp-Leu-Ain-OMe	62.5	30.5	−65.7	−48.1	53.5	39.8	32
For-Met-Dpg-Phe-OMe	−75.8	−30.4	173.1	179.0	−96.7	33.6	7
For-Met-Δ^zLeu-Phe-OMe	−55	129.7	72.2	14.3	−50.4	137.2	33
For-Met-Leu-D-(αMe)Phe-OMe	−105.1	136.3	−140.5	111.4	45.2	49.2	34
For-Hse(Me)-Leu-Phe-OMe	−143.8	121.9	−93.3	116.7	−94.8	29.0	10
For-Thp-LeuΔ^zPhe-OMe	−52.9	−32.8	−74.3	−9.6	63.7	−170.0	35
For-Thp-Ac_6c-Phe-OMe	−63.1	−33.9	52.2	51.2	−62.5	149.1	36
For-Met-Dmt-Phe-OMe	−162.0	154.7	−179.0	171.7	−74	−32	This paper

[a] Highly extended backbone fragments are evidenced.
[b] Two independent molecules have been found in the asymmetric unit of the crystal.

cine residues containing acyclic side chains longer than a methyl group to stabilize fully extended (C_5) backbone conformations strongly suggests that this type of conformation plays a significant role in the receptor activation. It should be noted, however, that f MLP-OMe analogues adopting folded backbone conformations, due to the incorporation of cyclic[19] and asymmetrically $C^{\alpha,\alpha}$-dialkylsubstituted glycine residues,[37] do show chemotactic activity. These findings can be interpreted by admitting the operativity of an induced fit mechanism or the existence of equivalent spatial orientations of the side chains inside different backbone conformations. The reduced conformational flexibility of peptides containing sterically constrained residues suggests that the latter hypothesis should be prevalent.

EXPERIMENTAL PROCEDURES

Peptide Synthesis

Melting points were determined with a Büchi oil apparatus and are uncorrected. Optical rotations were taken at 20°C with a Schmidt-Haensch Polartronic D polarimeter in a 1 dm cell ($CHCl_3$). Infrared spectra were recorded with a Perkin-Elmer 983 spectrophotometer (KBr disks, unless otherwise noted) and with a Perkin-Elmer 16FPC Fourier transform ir spectrophotometer ($CHCl_3$ solution; 0.5, 2, and 3 mm CsI cells). ^{1}H-nmr spectra were measured with a Varian XL-300 spectrometer in $CDCl_3$ (tetramethylsilane as internal standard). Column chromatographies were carried out using Merck silica gel 60 (230–400 mesh; 1:40). Thin-layer and preparative layer chromatographies (plc) were performed on silica gel Merck 60 F_{254} plates. The drying agent was sodium sulfate. Analytical data: Servizio Microanalisi del CNR, Area della Ricerca di Roma, Montelibretti, Italy. The parent f MLP-OMe was prepared according to Ref. 38.

Boc-Dmt-Phe-OMe

To a chilled solution of Boc-Dmt-OH[5] (0.223 g, 0.69 mmol) and HOBt (0.099 g, 0.69 mmol) in dry dichloromethane (2.8 mL) EDC (0.132 g, 0.69 mmol) was added. The mixture was kept at −5°C for 10 min, at room temperature for 20 min, and then a cold solution of HCl · H-Phe-OMe (0.148 g, 0.69 mmol) in dry *N*,*N*-dimethylformamide (1.4 mL) neutralized with *N*,*N*-diisopropylethylamine was added dropwise. A further amount of EDC (0.067 g) was added and the mixture was stirred at room temperature for 70 h. The solvent was removed under reduced pressure and the residue was dissolved in ethyl acetate, washed with 5% aqueous $KHSO_4$, water, saturated aqueous $NaHCO_3$, and brine. The organic phase was dried and evaporated to give a residue that was chromatographed on a silica gel column. Elution with *n*-hexane-ethyl acetate (9:1) afforded the title dipeptide (0.185 g, 55%) as an oil, $[\alpha]_D$ + 7° (*c* 1.0); R_f: 0.45 in *n*-hexane-ethyl acetate (8:2); ir ($CHCl_3$): 3401, 1741, 1704, 1672 cm^{-1}; nmr: δ 1.41 [9H, s, $C(CH_3)_3$], 1.63–2.70 (8H, m, two CH_2-CH_2-S), 2.00 and 2.04 (6H, two s, two S-CH_3), 3.03 and 3.19 (2H, A and B of an ABX, J = 5.3, 7.8 and 14 Hz, Phe β-CH_2), 3.74 (3H, s, $COOCH_3$), 4.90 (1H, m, Phe α-CH), 5.76 (1H, s, Dmt NH), 6.43 (1H, d, J = 7.8 Hz, Phe NH), 7.12–7.37 (5H, m, aromatic).

Boc-Met-Dmt-Phe-OMe

The title tripeptide was prepared following the procedure described above starting from Boc-Met-OH (0.095 g, 0.382 mmol) and TFA·H-Dmt-Phe-OMe (0.382 mmol) obtained by acidolysis of Boc-Dmt-Phe-OMe with TFA-$CHCl_3$.[32] The usual workup gave a residue that was chromatographed on a silica column, eluting with *n*-hexane-ethyl acetate (95:5). Further purification by plc [*n*-hexane-ethyl acetate (1:1) as eluant] afforded pure Boc-Met-Dmt-Phe-OMe (0.082 g, 35%), mp 119–120°C (from ethyl acetate-*n*-hexane); $[\alpha]_D$ −7° (*c* 0.7); R_f: 0.50 in *n*-hexane-ethyl acetate (1:1); ir: 3381, 3294, 1711, 1677, 1641 cm^{-1}; nmr: δ 1.44 [9H, s, $C(CH_3)_3$], 1.64–2.82 [12 H, m, two Dmt CH_2-CH_2-S, Met β-CH_2, and Met γ-CH_2 (t at 2.55, J = 7.2 Hz)], 2.00 and 2.02 (6H, two s, two Dmt S-CH_3), 2.10 (3H, s, Met S-CH_3), 3.04 and 3.21 (2H, A and B of an ABX, J = 5.5, 8 and 14 Hz, Phe β-CH_2), 3.75 (3H, s, $COOCH_3$), 4.17 (1H, m, Met α-CH), 4.89 (1H, m, Phe α-CH), 5.14 (1H, d, J = 7.6 Hz, Met NH), 6.42 (1H, d, J = 7.5 Hz, Phe NH), 7.12–7.36 (5H, m, aromatic), 7.40 (1H, s, Dmt NH).

Anal. Calc. for $C_{28}H_{45}N_3O_6S_3$: C 54.60, H 7.37, N 6.82%. *Found:* C 54.78, H 7.32, N 6.76%.

Attempt to improve the yield of the title tripeptide via *O*-(benzotriazol-1-yl)-*N*,*N*,*N*′,*N*′-bis(tetramethylene)-uronium hexafluorophosphate (HBPyU) carboxy-activation[39] have been unsuccessful.

HCO-Met-Dmt-Phe-OMe (2)

Boc-Met-Dmt-Phe-OMe (0.160 g, 0.259 mmol) was dissolved in 99% formic acid (1.04 mL) and stirred at room temperature for 24 h. After removal of the excess of formic acid in vacuo, the residue was dissolved in dry chloroform (1.04 mL) and EEDQ (0.077 g, 0.311 mmol) was added. The solution was stirred at room temperature for 5 h and *n*-hexane was added. The crude oil obtained was washed several times with ether and dried to give pure title *N*-formyltripeptide **2** (0.133 g, 94%), mp 129.5–130.5°C (from ethyl acetate-*n*-hexane); $[\alpha]_D$ −10° (*c* 1.0); R_f: 0.42 in *n*-hexane-ethyl acetate (3:7); ir: 3348, 3275, 1723, 1678, 1643, 1529 cm^{-1}; nmr: δ 1.70–2.79 (12 H, m, two Dmt CH_2-CH_2-S, and Met CH_2-CH_2-S), 2.00 and 2.02 (6H, two s, two Dmt S-CH_3), 2.11 (3H, s, Met S-CH_3), 3.05 and 3.21 (2H, A and B of an ABX, J = 5.2, 8 and 14 Hz, Phe β-CH_2), 3.76 (3H, s, $COOCH_3$), 4.62 (1H, m, Met α-CH), 4.89 (1H, m, Phe α-CH), 6.34 (2H, m, Met and Phe NH), 7.12–7.39 (5H, m, aromatic), 7.34 (1H, s, Dmt NH), 8.19 (1H, s, HCO).

Anal. Calc. for $C_{24}H_{37}N_3O_5S_3$: C 53.01, H 6.86, N 7.73%. *Found:* C 52.92, H 6.91, N 7.44%.

Boc-Dmt-Leu-Phe-OMe

The title tripeptide was prepared following the procedure described above for Boc-Met-Dmt-Phe-OMe, starting from Boc-Dmt-OH[5] (0.165 g, 0.51 mmol) and TFA·H-Leu-Phe-OMe[32] (0.51 mmol). The reaction was carried out for 45 h and usual workup afforded a residue that was chromatographed on a silica column. Elution with dichloromethane-ether (95:5) afforded pure Boc-tripeptide (0.18 g, 59%), mp 91–92°C (from ethyl acetate-*n*-hexane); $[\alpha]_D$ + 13° (*c* 1.0); R_f: 0.52 in dichloromethane-ethyl acetate (8:2); ir: 3354, 3271, 1747, 1712, 1641 cm^{-1}; nmr: δ 0.89 [6H, apparent t, $CH(CH_3)_2$], 1.43 [9H, s, $C(CH_3)_3$], 1.46–1.65 [3H, m, CH_2-$CH(CH_3)_2$], 1.90–2.57 (8H, m, two CH_2-CH_2-S), 2.06 (6H, s, two S-CH_3), 3.10 (2H, m, Phe β-CH_2), 3.70 (3H, s, $COOCH_3$), 4.37 (1H, m, Leu α-CH), 4.73 (1H, m, Phe α-CH), 5.66 (1H, s, Dmt NH), 6.49 (1H, d, J = 7.6 Hz, Phe NH), 6.54 (1H, d, J = 7.8 Hz, Leu NH), 7.09–7.33 (5H, m, aromatic).

Anal. Calc. for $C_{29}H_{47}N_3O_6S_2$: C 58.26, H 7.92, N 7.03%. *Found:* C 58.01, H 7.77, N 6.70%.

HCO-Dmt-Leu-Phe-OMe (3)

The formyl derivative **3** was prepared following the usual formylation procedure, starting from Boc-Dmt-Leu-Phe-OMe (0.18 g, 0.301 mmol). The crude product, precipitated by *n*-hexane, was purified by plc (ethyl acetate as eluant) to afford pure title compound **3** (0.114 g, 72%), mp 99–100°C (from ethyl acetate-*n*-hexane); $[\alpha]_D$ + 28° (*c* 0.8); R_f: 0.62 in dichloromethane-ethyl acetate (2:8); ir: 3318, 1746, 1642 cm^{-1}; nmr: δ 0.92 [6H, m, $CH(CH_3)_2$], 1.51–1.67 [3H, m, CH_2-$CH(CH_3)_2$], 1.84–2.98 (8H, m, two CH_2-CH_2-S), 2.05 and 2.07 (6H, two s, two S-CH_3), 3.12 (2H, m, Phe β-CH_2), 3.74 (3H, s, $COOCH_3$), 4.39 (1H, m, Leu α-CH), 4.81 (1H, m, Phe α-CH), 6.29 (1H, d, J = 7.3 Hz, Phe NH), 6.46 (1H, d, J = 7.5 Hz, Leu NH), 6.95 (1H, s, Dmt NH), 7.08–7.34 (5H, m, aromatic), 8.21 (1H, s, HCO).

Anal. Calc. for $C_{25}H_{39}N_3O_5S_2$: C 57.11, H 7.48, N 7.99%. *Found:* C 57.21, H 7.60, N 7.90%.

X-Ray Data Collection and Reduction

Crystals of **2** were obtained from dry benzene by slow evaporation. The x-ray data were collected at room temperature on a Rigaku AFC5R diffractometer with graphite monochromated Cu-kα radiation and a 6KW rotating anode generator. Cell constants, space group, and an orientation matrix for data collection were obtained from a least-squares fit of the angular settings of 15 carefully centered reflections in the range $30° < 2\theta < 50°$. The cell parameters, refined on higher angle reflections, are reported in Table III. Intensity data were collected by the $\omega/2\theta$ technique, with a scan width of $(1.4 + 0.3\mathrm{tg}\theta)°$ at a variable and appropriate speed to a maximum 2θ of 124°. Stationary background counts were recorded on each side of the reflection. The peak counting time was twice that of the background. Reflections with $I < 10\sigma(I)$ were rescanned with an accumulation of counts to improve counting statistics. Out of 3425 collected reflections, 2246 had $I > 3\sigma(I)$ and were considered observed.

Table III Crystal Data of 2

Empirical formula	$C_{24}H_{37}N_3O_5S_3 \cdot 2C_6H_6$
Formula weight	700
Crystal system	Monoclinic
a(Å)	14.175 (3)
b (Å)	10.432 (1)
c (Å)	14.401 (4)
β (°)	113.51 (1)
V (Å^3)	1953 (2)
Space group	$P2_1$
D_c(g cm^{-3})	1.19
Z	2
F(000)	748
λ(Cu-Kα) (Å)	1.5418
μ(Cu-Kα) (mm^{-1})	2.0
Crystal size (mm)	0.1 × 0.5 × 0.04
$2\theta_{max}$ (°)	124
Reflections with $I > 3\sigma(I)$	2246
R, R_w	0.095, 0.103
Weighting scheme	$K_1[\sigma^2(F_0) + K_2F_0^2]^{-1}$
S	1.5
Observations/parameter	6.1

The intensities of three standard reflections measured after every 150 reflections remained constant throughout data collection indicating crystal and electronic stability. An empirical absorption correction, based on azimuthal scans of several reflections, was applied. The data were finally corrected for Lorentz and polarization effects.

Structure Solution and Refinement

The structure of **2** was solved by direct methods using the program SIR[40] and successive Fourier maps. Full matrix least-squares refinement was carried out using the program SHELX 76.[41] The function minimized was $\Sigma w(|F_0| - |F_c|)^2$ where $w = k_1[\sigma^2(F_0) + k_2F_0^2]^{-1}$, k_1 and k_2 being two constants redetermined after each cycle. Since the geometry of the two cocrystallized benzene molecules assumed unexpected values, it was decided to treat them as rigid groups. Regular hexagons with C—C bond lengths of 1.395 Å and C—C—C angles of 120° were fitted to their carbons, which were refined only isotropically. A difference Fourier map revealed two additional peaks around the terminal part of the Met side chain that were interpreted as the sulfur and methyl carbon of a minor conformation of the Met side chain. An occupancy factor of $\frac{1}{3}$ was assigned to these two atoms that were refined only isotropically. All other non-H atoms of the peptide were refined anisotropically. Riding H atoms were included in the refinement with positional parameters at expected positions (C—H = 1.09 Å, N—H = 1.00 Å) and isotropic thermal parameters deduced from the carrier atoms. The final R and R_w are 0.095 and 0.103, respectively. The scattering factors were those of Cromer and Mann.[42] The correction for the real and imaginary parts of the anomalous dispersion was taken into account for the S atoms. The final fractional coordinates of the non-H atoms together with their B_{eq} and individual e.s.d.'s, the anisotropic thermal parameters of the non-H atoms, bond lengths, valence angles, observed, and calculated structure factors are available on request from the authors. All the calculations were performed on a Digital VAX station 3100.

Biological Assay

Cells. Human peripheral blood neutrophils were purified employing the standard techniques of dextran (Pharmacia) sedimentation, centrifugation on Ficoll-Paque (Pharmacia), and hypotonic lysis of red cells. The cells were washed twice and resuspended in KRPG (Krebs-Ringer phosphate containing 0.1% w/v glucose, pH 7.4) at a concentration of 50 × 10^6 cells/mL. Neutrophils were 98–100% pure.

Random Locomotion. Random locomotion was performed with 48-well microchemotaxis chamber (Bio Probe, Italy) and the migration into the filter was evaluated by the method of leading-front.[43] The actual control random movement is 32 μm ± 3 SE of ten separate experiments done in duplicate.

Chemotaxis. In order to study the potential chemotactic activity, each peptide was added to the lower compartment of the chemotaxis chamber. Peptides were diluted from a stock solution ($10^{-2}M$ in DMSO) with KRPG containing 1 mg/mL of bovine serum albumin (Orha Behringwerke, FRG) and used at concentrations ranging from 10^{-12} to $10^{-5}M$. Data were expressed in terms of chemotactic index, which is the ratio (migration toward test attractant minus migration toward the buffer)/migration toward the buffer.

Superoxide Anion (O_2^-) Production. O_2^- release was monitored continuously in a thermostatted spectrophotometer as superoxide dismutase-inhibitable reduction of ferricytochrome c (Sigma, USA), as described elsewhere.[44] At zero time, different amounts (10^{-9} to 2 × $10^{-5}M$) of each peptide were added and absorbance change accompanying cytochrome c reduction was monitored at 550 nm. Neutrophils were incubated with 5 μg/mL cytochalasin B (Sigma) for 5 min prior to activation by peptides. Results were expressed as net nmoles of $O_2^-/2 \times 10^6$ cells/5 min and are the mean of six separate experiments done in duplicate.

Enzyme Assay. Release of neutrophil granule enzymes was evaluated by determining lysozyme activity[44]; this was quantified nephelometrically by the rate of lysis of a cell wall suspension of *Micrococcus lysodeikticus* (Sigma). Enzyme release was expressed as a net percentage of total enzyme content released by 0.1% Triton X-100. Total enzyme activity was 85 ± 1 μg/1 × 10^7 cells/

min. To study the degranulation-inducing activity of each peptide, neutrophils were first incubated with cytochalasin B for 15 min at 37°C and then in the presence of each peptide in a final concentration of 10^{-9} to $2 \times 10^{-5} M$ for a further 15 min.

Statistical Analysis. The nonparametric Wilcoxon test was used in the statistical evaluation of differences between groups.

This work was supported in part by MURST. We are grateful to Banca del Sangue of Ferrara for providing fresh blood. Drawings by Mr. Trabassi.

REFERENCES

1. Toniolo, C. & Benedetti, E. (1991) *Macromolecules* **24,** 4004–4009.
2. Balaram, P. (1992) *Curr. Opin. Struct. Biol.* **2,** 845–851.
3. Toniolo, C. (1993) *Janssen Chim. Acta* **11,** 10–16.
4. Sudhanand Prasad, Balaji Rao, R. & Balaram, P. (1995) *Biopolymers* **35,** 11–20.
5. Torrini, I., Paglialunga Paradisi, M., Pagani Zecchini, G. & Lucente, G. (1994) *Synth. Commun.* **24,** 153–158.
6. Crisma, M., Valle, G., Bonora, G. M., Toniolo, C., Lelj, F., Barone, V., Fraternali, F., Hardy, P. M. & Maia, H. L. S. (1991) *Biopolymers* **31,** 637–641.
7. Dentino, A. R., Raj, P. A., Bhandary, K. K., Wilson, M. E. & Levine, M. J. (1991) *J. Biol. Chem.* **266,** 18460–18468.
8. Sauvé, G., Rao, V. S., Lajoie, G. & Belleau, B. (1985) *Can. J. Chem.* **63,** 3089–3101.
9. Lajoie, G. & Kraus, J. L. (1984) *Peptides* **5,** 653–654.
10. Torrini, I., Pagani Zecchini, G., Paglialunga Paradisi, M., Lucente, G., Gavuzzo, E., Mazza, F., Pochetti, G., Traniello, S. & Spisani, S. (1994) *Biopolymers* **34,** 1–9.
11. Benedetti, E., Barone, V., Bavoso, A., Di Blasio, B., Lelj, F., Pavone, V., Pedone, C., Bonora, G. M., Toniolo, C., Leplawy, M. T., Kaczmarek, K. & Redlinski, A. (1988) *Biopolymers* **27,** 357–371.
12. Benedetti, E., Morelli, G., Nemethy, G. & Scheraga, H. A. (1983) *Int. J. Peptide Protein Res.* **22,** 1–15.
13. Gould, R. O., Gray, A. M., Taylor, P. & Walkinshaw, M. D. (1985) *J. Am. Chem. Soc.* **107,** 5921–5927.
14. Ashida, T., Tsunogae, Y., Tanaka, I. & Yamane, T. (1987) *Acta Cryst.* **B43,** 212–218.
15. Crisma, M., Valle, G., Bonora, G. M., De Menego, E., Toniolo, C., Lelj, F., Barone, V. & Fraternali, F. (1990) *Biopolymers* **30,** 1–11.
16. Toniolo, C., Crisma, M., Fabiano, N., Melchiorri, P., Negri, L., Krause, J. A. & Eggleston, D. S. (1994) *Int. J. Peptide Protein Res.* **44,** 85–95.
17. Inai, Y., Ito, T., Hirabayashi, T. & Yokota, K. (1993) *Biopolymers* **33,** 1173–1184.
18. Bardi, R., Piazzesi, A. M., Toniolo, C. & Balaram, P. (1986) *Biopolymers* **25,** 1635–1644.
19. Toniolo, C., Crisma, M., Valle, G., Bonora, G. M., Polinelli, S., Becker, E. L., Freer, R. J., Sudhanand, R., Balaji Rao, R., Balaram, P. & Sukumar, M. (1989) *Peptide Res.* **2,** 275–281.
20. Bardi, R., Piazzesi, A. M., Toniolo, C., Sukumar, M., Raj, P. A. & Balaram, P. (1985) *Int. J. Peptide Protein Res.* **25,** 628–639.
21. Raj, P. A. & Balaram, P. (1985) *Biopolymers* **24,** 1131–1146.
22. Freer, R. J., Day, A. R., Radding, J. A., Schiffmann, E., Aswanikumar, S., Showell, H. J. & Becker, E. L. (1980) *Biochemistry* **19,** 2404–2410.
23. Edmundson, A. B. & Ely, K. R. (1985) *Mol. Immunol.* **22,** 463–475.
24. Wang, C.-R., Castaño, A. R., Peterson, P. A., Slaughter, C., Fischer Lindahl, K. & Deisenhofer, J. (1995) *Cell* **82,** 655–664.
25. Wu, A., Muthukumaraswamy, N., Glasel, J. A., Mackin, W. M., Becker, E. L. & Freer, R. J. (1983) *FEBS Lett.* **159,** 150–152.
26. Toniolo, C., Crisma, M. & Becker, E. L. (1990) *Il Farmaco* **45,** 921–925.
27. Pagani Zecchini, G., Paglialunga Paradisi, M., Torrini, I., Lucente G., Traniello, S. & Spisani, S. (1993) *Arch. Pharm.* (Weinheim) **326,** 461–465.
28. Gavuzzo, E., Mazza, F., Pochetti, G. & Scatturin, A. (1989) *Int. J. Peptide Protein Res.* **34,** 409–415.
29. Michel, A. G., Lajoie, G. & Hassani, C. A. (1990) *Int. J. Peptide Protein Res.* **36,** 489–498.
30. Gavuzzo, E., Lucente, G., Mazza, F., Pagani Zecchini, G., Paglialunga Paradisi, M., Pochetti, G. & Torrini, I. (1991) *Int. J. Peptide Protein Res.* **37,** 268–276.
31. Toniolo, C., Crisma, M., Pegoraro, S., Valle, G., Bonora, G. M., Becker, E. L., Polinelli, S., Boesten, W. H. J., Schoemaker, H. E., Meijer, E. M., Kamphuis, J. & Freer, R. J. (1991) *Peptide Res.* **4,** 66–71.
32. Torrini, I., Pagani Zecchini, G., Paglialunga Paradisi, M., Lucente, G., Gavuzzo, E., Mazza, F., Pochetti, G., Spisani, S. & Giuliani, A. L. (1991) *Int. J. Peptide Protein Res.* **38,** 495–504.
33. Pagani Zecchini, G., Paglialunga Paradisi, M., Torrini, I., Lucente, G., Gavuzzo, E., Mazza, F., Pochetti, G., Paci, M., Sette, M., Di Nola, A., Veglia, G., Traniello, S. & Spisani, S. (1993) *Biopolymers* **33,** 437–451.
34. Toniolo, C., Formaggio, F., Crisma, M., Valle, G., Boesten, W. H. J., Schoemaker, H. E., Kamphuis, J., Temussi, P. A., Becker, E. L. & Précigoux, G. (1993) *Tetrahedron* **49,** 3641–3653.
35. Torrini, I., Pagani Zecchini, G., Paglialunga Paradisi, M., Lucente, G., Gavuzzo, E., Mazza, F., Pochetti, G., Traniello, S., Spisani, S. & Cerichelli, G. (1994) *Biopolymers* **34,** 1291–1302.
36. Torrini, I., Pagani Zecchini, G., Paglialunga Paradisi, M., Lucente, G., Mastropietro, G., Gavuzzo, E.,

Mazza, F., Pochetti, G., Traniello, S. & Spisani, S. (1996) *Biopolymers* **39,** 327–337.
37. Formaggio, F., Pantano, M., Crisma, M., Toniolo, C., Boesten, W. H. J., Schoemaker, H. E., Kamphuis, J. & Becker, E. L. (1993) *BioMed. Chem. Lett.* **3,** 953–956.
38. Vertuani, G., Spisani, S., Boggian, M., Traniello, S. & Scatturin, A. (1987) *Int. J. Peptide Protein Res.* **29,** 525–532.
39. Chen, S. & Xu, J. (1992) *Tetrahed. Lett.* **33,** 647–650.
40. Burla, M. C., Camalli, M., Cascarano, G., Giacovazzo, C., Polidori, G., Spagna, R. & Viterbo, D. (1989) *J. Appl. Cryst.* **22,** 389–393.
41. Sheldrick, G. M. (1976) *SHELX 76: A Program for Crystal Structure Determination,* University of Cambridge, England.
42. Cromer, D. T. & Mann, J. B. (1968) *Acta Cryst.* **A24,** 321–324.
43. Zigmond, S. H. & Hirsch, J. G. (1973) *J. Exp. Med.* **137,** 387–410.
44. Spisani, S., Giuliani, A. L., Cavalletti, T., Zaccarini, M., Milani, L., Gavioli, R. & Traniello, S. (1992) *Inflammation* **16,** 147–157.